



SORBONNE UNIVERSITÉ

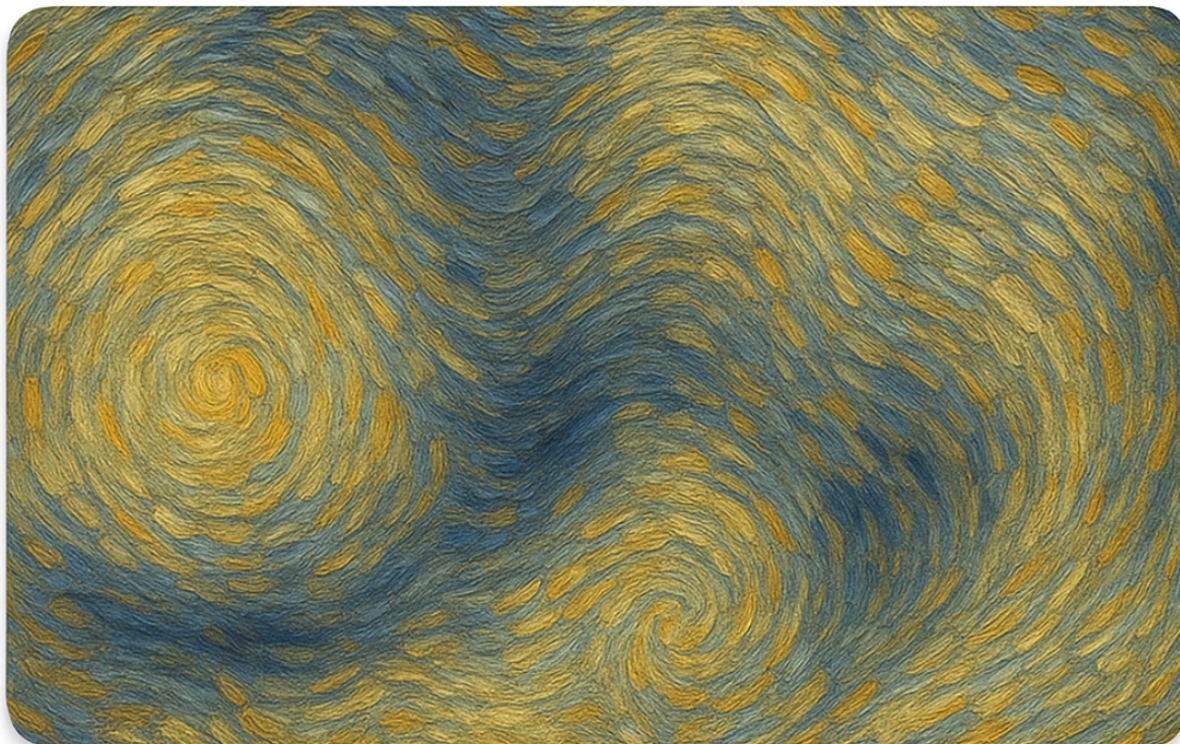
MASTER OF PHYSICS - 2nd YEAR

2024-2025

MASTER REPORT

Quantum effect in paraxial fluid of light

ALEXANDRE LEVAIN



Laboratory :
Laboratoire Kastler-Brossel

Supervisor :
Quentin Glorieux

Status :
Professor

Table des matières

1 Internship framework and thanks	2
2 Interests of fluid of light	3
3 Propagation in nonlinear medium	4
3.1 Mapping with GPE	6
3.2 Dimensionless equation and comparison with cold atoms	7
4 Bogoliubov theory	7
5 How to see a fluid in experiment	9
5.1 Off-axis interferometry	9
6 First steps in the lab	10
6.1 Rubidium cell	11
6.2 Off-axis interferometry experiment	12
7 Measurement of the nonlinear index	13
7.1 Measurement protocol	13
7.2 Analysis protocol	14
8 Quantum effects	15
8.1 Beyond mean-field	15
8.2 Four-wave-mixing process	15
8.3 Input-output approach	16
9 Theoretical description of correlations in momentum space	18
9.1 Theoretical description of the spontaneous-four-wave mixing	18
9.2 Correlation in far-field regime	19
9.3 A good observable $\hat{N}(\mathbf{k}_\perp)$	20
9.4 Measurement protocol	20
9.5 Experimental set-up to probe the population	20
9.6 Analysis protocol	21
9.7 Preliminary results and perspectives	21
10 Conclusion	22
A Discussion about the observable $\hat{N}(\mathbf{k}_\perp)$	25
B Quantum physic in experiment	25
B.1 Mean value of an observable	25
B.2 Statistical approach of correlations	26
C Python codes	27

1 Internship framework and thanks

I completed my Master's 2 internship in physics at the Laboratoire Kastler Brossel (LKB), coordinated by Quentin Glorieux and his doctoral students.

The Kastler Brossel Laboratory is a multidisciplinary laboratory specialized in fundamental physics of quantum systems. It is made up of 180 members spread across three locations : Collège de France, Ecole Normale Supérieure and Sorbonne Université which welcomes the quantum fluid of light team. I was a member of this team from March 10th to August 1st of 2025.

During this period, I have deepened my knowledge in different domains : quantum fluids, quantum optics, and experimental physics. Having easy access to the lab and to scientific equipment was a fantastic opportunity that helped me enjoy studying physics even more. This internship allowed me to better understand the physics of fluid of light and to better grasp theoretical principles through practical application.

I would like to thank Quentin Glorieux, without whom this internship would never have been possible, as well as the whole team of quantum fluids of light in atom vapor team. This team is directed by Quentin Glorieux and is composed of two postdoc Devang Naik and Noémie Marquet and several Ph.D. students : Quentin Schibler, Clara Piekarski, Simon Lepleux, Myrann Baker-Rasooli, Alix Merolle and Sukhman Kler. A team with which I enjoyed working and who guided me in the world of research. In addition, we hold a weekly group meeting that allows me to ask questions and understand each other's work. Also, I thank the entire laboratory for their warm welcome.

I chose to apply to this internship in the domain of quantum fluid of the paraxial regime because I particularly appreciate this domain, which joins several branches of physics that I enjoy : optics, quantum mechanics, and cold atoms.

The aim of the project was to investigate the effect of quantum fluctuations in a photon condensate.

This phenomenon is known as quantum depletion in the Bose-Einstein condensate language. This effect reflects the fact that a certain number of particles leave the condensate due to interactions. This phenomenon was never studied before in the domain of quantum fluids of light. Therefore, my work focused on a mapping of quantum depletion for our system in quantum optics language and on finding good observables in the perspective to measure quantum properties of fluids of light.

2 Interests of fluid of light

The team strives to focus its research on fluid of light in paraxial regime. This study is the intersection between an abundant number of research topics : atom-light interactions, Bose-Einstein gases, fluid mechanics, quantum optics, etc.

During this report, topics related to the creation of a light fluid, quantum optic, and the study of weakly interacting Bose gases will be highlighted.

Paraxial fluids of light are a promising platform for exploring collective phenomena in a highly tunable environment. These systems, which map the propagation of light through non-linear media onto the wavefunction of effective 2D quantum fluids, offer a complementary approach to traditional platforms such as cold atomic gases or super-fluid helium. This property comes from the fact that fluid of light follows the nonlinear Schrödinger equation (NLSE) which can be mapped onto the Gross-Pitaevskii equation (GPE) describing the evolution of Bose gases wave function. This equation appears in the field of condensed matter and cold atoms [1], in plasmas physics [2], in nonlinear optics [3] , in fluid mechanic [4] etc. NLSE universalizes physics governed by a system with complex processes thanks to the non-linear part of the equation.

In particular, in the domain of optics, the NLSE describes the evolution of the electric field envelope through a third-order nonlinear medium. This type of evolution appears for different configurations : propagation in fiber [5] (where the beam is pulsed and propagates in one spatial dimension and in time, we talk about a $1D + 1$ system) and in the transverse plan in a non-linear medium , a $2D + 1$ system [6]. The second configuration will be our subject of interest.

The correspondence with the GPE that describes temporal evolution of a dilute Bose Einstein condensate (BEC) [7] allows us to study analogously cold atoms physics such as vortex generation, solitons [8], superfluid regime [9], quantum turbulence [10].

Moreover, these experiments are less restrictive to set up than those with cold atoms. Furthermore, cold atoms it is tricky to have access to amplitude and phase simultaneously.

3 Propagation in nonlinear medium

In this section, we will focus on the propagation of an electric field through a non-linear medium to obtain NLSE, with the aim of highlighting the fluid character of light in the paraxial regime. Moreover, we will draw parallels with the Gross-Pietavskii equation.

In a vacuum, photons don't interact with each other. But in $\chi^{(3)}$ non-linear medium, the Kerr effect (self-focusing or defocusing) can be interpreted as a attractive or a repulsive photon-photon interaction. This non-linearity can be observed in semiconductors where the fluid is exciton-polariton [11].

In an atomic vapor cell, the fluid describes directly the behavior of photons through the cell. The classical description of this quantum fluid is given by the so-called Non-Linear Schrödinger Equation 2 (NLSE). It can be obtained from the non-linearity of the polarization in the D'Alembert equation.

By decoupling Maxwell's equations, we obtain the propagation equation for the electric field $\mathbf{E}(\mathbf{r}, t)$, the polarization field $\mathbf{P}(\mathbf{r}, t)$ appears as a source term in the D'Alembert equation.

$$\nabla^2 \mathbf{E} - \frac{1}{c^2} \frac{\partial^2}{\partial t^2} \mathbf{E} = \frac{1}{\epsilon_0 c^2} \frac{\partial^2 \mathbf{P}}{\partial t^2} \quad (1)$$

with c celerity of light and ϵ_0 permittivity in vacuum.

Polarization \mathbf{P} translates the response to an electromagnetic excitation \mathbf{E} . This polarization can be expanded in a power serie of \mathbf{E} :

$$\mathbf{P}(\mathbf{r}, t) = \epsilon_0 \sum_n \chi^{(n)} \mathbf{E}^n(\mathbf{r}, t)$$

$\chi^{(n)}$ is n-order the electric susceptibility tensor.

The linearly polarized electric field propagates inside a cell composed of rubidium vapor. This medium is isotropic and centrosymmetric, so the expression of the polarization becomes simpler : $\chi^{(n)}$ is a scalar and the 2-order is null.

We now introduce the fundamental approximation that drive the geometry of the paraxial fluid.

The slowly varying envelope approximation : the variation of the amplitude in the direction of propagation z is weak at the wave length scale. Then we can neglect the second derivative of the field. $\frac{\partial^2 \mathcal{E}}{\partial z^2} \ll k \frac{\partial \mathcal{E}}{\partial z}$ where k is the wave vector.

We obtain the evolution equation of the envelope field \mathcal{E} , called Non-linear Schrödinger equation :

$$i \frac{\partial \mathcal{E}}{\partial z} = \underbrace{-\frac{1}{2k_0} \nabla_{\perp}^2 \mathcal{E} + \frac{D_0}{2} \frac{\partial^2 \mathcal{E}}{\partial t^2}}_{\text{Kinetic energy}} - \underbrace{\frac{i}{v_g} \frac{\partial \mathcal{E}}{\partial t}}_{\text{Drift}} - \underbrace{k_0 \frac{\delta n(\mathbf{r})}{n_0} \mathcal{E}}_{\text{Potential}} - \underbrace{k_0 \frac{n_2}{n_0} |\mathcal{E}|^2 \mathcal{E}}_{\text{Interaction}} - i \underbrace{\frac{\alpha}{2} \mathcal{E}}_{\text{Losses}} \quad (2)$$

In addition, to illustrating the NLSE terms fig.2, we will discuss the physical meaning of each terms.

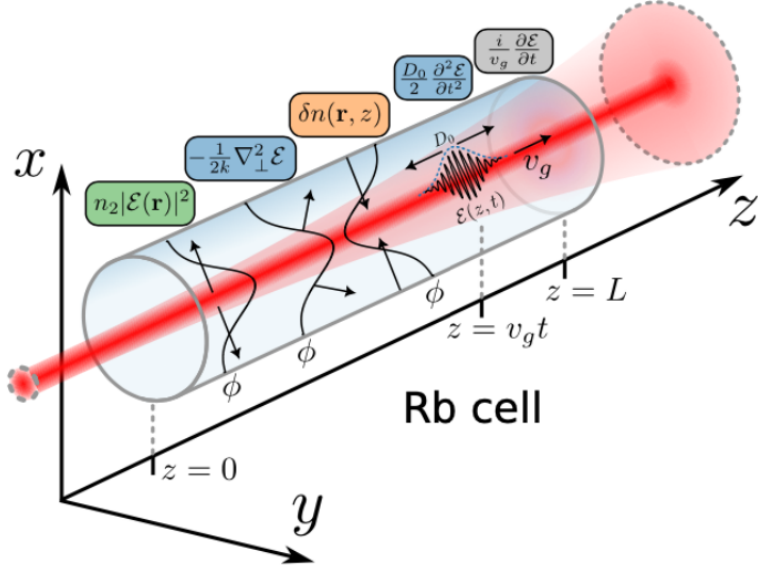


FIGURE 1 – Effect of the different terms in NLSE, extracted from [12]

Kinetic energy : This term translates the wavefront curvature in the plane (x,y) and the dispersion along z . The first comes from diffraction and the second represents group velocity dispersion. We can define an effective mass for the photons : transverse mass $m_\perp = k_0$ and longitudinal mass $m_t = -\frac{1}{D_0}$ with k_0 the wave vector and D_0 the group velocity dispersion.

Potential : It is possible to create an arbitrary potential by locally modifying the linear refractive index. In warm atomic vapors, one can exploit the hyperfine structure of atomic levels to optically pump atoms into a dark state. It can reduce the effective density of atoms and thus locally modify the index of refraction.

Interaction : This is the so-called Kerr term that creates photon-photon interaction. The latter is often described by a variation in the index of refraction Δn . This index can be easily adjusted by changing the intensity of the field and the third-order susceptibility. In the case of a non-linear index of refraction $n_2 < 0$, interactions are repulsive and the fluid is stable. In the other case, the beam focuses as much as it is intense, leading to the phenomenon of filamentation.¹

Losses : Absorption creates linear losses due to the imaginary part of the susceptibility. The intensity inside the cell follows the Beer-Lambert law. Moreover, the losses are considered to be negligible for a beam far from resonance. (not always experimental conditions)

Drift : This rigid drift comes from the difference in the group velocity in the medium and in the vacuum. This term can be easily removed thanks to a change of framework (by placing oneself in the pulse frame of reference) and is important for a pulse or a nonmonochromatic beam.

1. It is note, that far from resonance $\Delta \gg \Gamma$, where the laser detuning is large enough compared to the linewidth of the transition, the Kerr term scales as $\chi^{(3)} \propto \frac{N}{\Delta^3}$, which depends linearly on the atomic density N and is highly sensitive to detuning.

3.1 Mapping with GPE

Equation 2 looks like the Gross-Pietavskii equation (GPE) that describes the evolution of a macroscopic wave function ψ of a Bose gas in a BEC :

$$i\hbar \frac{\partial \psi}{\partial t} = \underbrace{\frac{\hbar^2}{2m} \nabla^2 \psi}_{\text{Kinetic energy}} + \underbrace{V\psi}_{\text{Potential}} + \underbrace{g|\psi|^2\psi}_{\text{Interaction}} \quad (3)$$

With \hbar the Planck constant divided by 2π , m the mass of a particle, V the potential et g the interaction parameter related to the scattering length.

To highlight the analogy, we will rewrite NLSE. To facilitate the description, we will consider the most simple case : a monochromatic field with no losses. The spatial dynamic appears only in the transverse plan and the kinetic energy also. Then equation 2 becomes :

$$i\frac{\partial \mathcal{E}}{\partial z} = -\underbrace{\frac{1}{2k_0} \nabla_{\perp}^2 \mathcal{E}}_{\text{kinetic energy}} - \underbrace{k_0 \frac{\delta n(\mathbf{r})}{n_0} \mathcal{E}}_{\text{Potential}} - \underbrace{k_0 \frac{n_2}{n_0} |\mathcal{E}|^2 \mathcal{E}}_{\text{Interaction}} \quad (4)$$

We can set the potential term as $V = -k_0 \frac{\delta n}{n_0}$ and the interaction term as $g = -k_0 \frac{n_2}{n_0}$.

Now, we can better see the similarity to GPE :

$$i\frac{\partial \mathcal{E}}{\partial z} = -\underbrace{\frac{1}{2k_0} \nabla_{\perp}^2 \mathcal{E}}_{\text{kinetic energy}} + \underbrace{V\mathcal{E}}_{\text{Potential}} + \underbrace{g|\mathcal{E}|^2\mathcal{E}}_{\text{Interaction}} \quad (5)$$

Finally, the only difference between the equations 5 and 3 is the spatial and temporal evolution of the quantity of interest. NLSE describes the spatial evolution of the electric field envelope and GPE describes the temporal evolution of the BEC wave function. So if we consider the propagation axis z as an effective time : NLSE is analogous to a 2D photon gas evolving in the transverse plan and the propagation axis describes the temporal evolution of the gas. We talk about a **2D+1** system fig.(2).

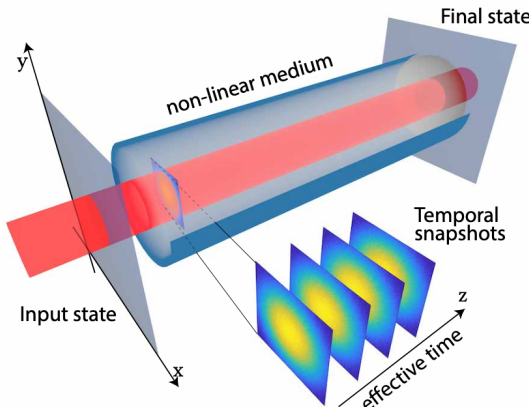


FIGURE 2 – Sketch of the 2D+1 paraxial fluid of light. A laser propagates along z in a nonlinear medium. Each transverse plane (x, y) is equivalent to a temporal snapshot. Input state is user-defined and the final state is measured experimentally, extracted from [12]

3.2 Dimensionless equation and comparison with cold atoms

To better understand the behaviour of a fluid of light. It is useful to provide a quantitative comparison between paraxial fluids of light and ultracold atomic Bose gases ; it is useful to adimensionalize the NLSE and the GPE. We rescale the transverse dynamics by the healing length : $\xi = \frac{1}{k_0 \sqrt{2|\Delta n|}}$ which is defined as the length scale where kinetic energy equals the interaction energy. To get an idea of this quantity, a short healing length corresponds to a significant local non-linear interaction, so the field envelope is strongly modified over a short distance.

We also introduce another characteristic length in the longitudinal direction, the non-linear length :

$$z_{NL} = \frac{1}{k_0 |\Delta n|}$$

It is the propagation length (or effective evolution time).

We make the following changes of variables : $\tilde{r}_\perp = \frac{r_\perp}{\xi}$, $\tilde{z} = \frac{z}{z_{NL}}$ and $\tilde{\psi} = \mathcal{E}/\sqrt{\frac{2I_0}{\epsilon_0 c}}$ where I_0 is the average intensity of the field.

Then, dropping the external potential for simplicity, the equation 5 becomes :

$$i \frac{\partial \tilde{\psi}}{\partial \tilde{z}} = (-\tilde{\nabla}_\perp^2 + |\tilde{\psi}|^2) \tilde{\psi}$$

With $\tilde{\nabla}_\perp$ the transverse normalized gradient. A similar adimensionalization can be done for the GPE describing a uniform BEC by defining the healing length $\xi = \frac{\hbar}{\sqrt{2m\mu}}$, the nonlinear time $t_{NL} = \frac{\hbar}{\rho g}$ and $\tilde{\psi} = \frac{\psi}{\sqrt{\rho_0}}$ where $\mu = g\rho_0$. ρ_0 is the average density of the condensate and μ is the chemical potential. Intuitively, the healing length describes how quickly the wave function of the BEC can adjust to changes in the potential.

Quantity	Optics 2D+1	BEC
Evolution	z in [m]	t in [s]
Mass	k_0 in $[m^{-1}]$	m in [kg]
Energies	in $[m^{-1}]$	in [J]
Kinetic energy	$\frac{k_\perp^2}{2k_0}$	$\frac{(\hbar k)^2}{2m}$
Potential	$-k_0 \frac{\delta n(r)}{n_0}$	$V(r)$
Interaction	$-k_0 \Delta n$	ρg
Healing length in [m]	$\xi = \frac{1}{k_0 \sqrt{2 \Delta n }}$	$\xi = \frac{\hbar}{\sqrt{2m\rho g}}$
Non-linear length	$z_{NL} = \frac{1}{k_0 \Delta n }$ in [m]	$t_{NL} = \frac{\hbar}{\rho g}$ in [s]

TABLE 1 – Comparison between NLSE and GPE parameters. The natural experimental units to express the energies are $[m^{-1}]$ in optics and [J] for atomic BEC

4 Bogoliubov theory

Equation (4) cannot be resolved exactly due to the presence of the nonlinear term. Nevertheless, we can treat this equation with a perturbative approach and conserve the terms until first order. Seeing as a development of the Bogoliubov theory can be long and tricky for a non-expert. I will bypass

this difficulty by giving the equations without demonstration. Nevertheless, I will discuss the physical meaning of the different equations.

Starting by considering small fluctuations on the field. The latter can be decomposed following mean field theory as :

$$\mathcal{E}(\mathbf{r}_\perp, z) = \langle \mathcal{E} \rangle + \delta\mathcal{E}(\mathbf{r}_\perp, z)$$

Where $\langle \mathcal{E} \rangle$ is the mean field and $\delta\mathcal{E}$ its fluctuations with $\langle \mathcal{E} \rangle \gg \delta\mathcal{E}$

By injecting this form of solution into the GPE equation and linearising, it can be shown that these fluctuations have a particular dispersion relation illustrated fig.(3).

$$\Omega_B(k_\perp) = \sqrt{\left(\frac{k_\perp^2}{2k_0} + 2k_\perp^2 |\Delta n|\right)} \quad (6)$$

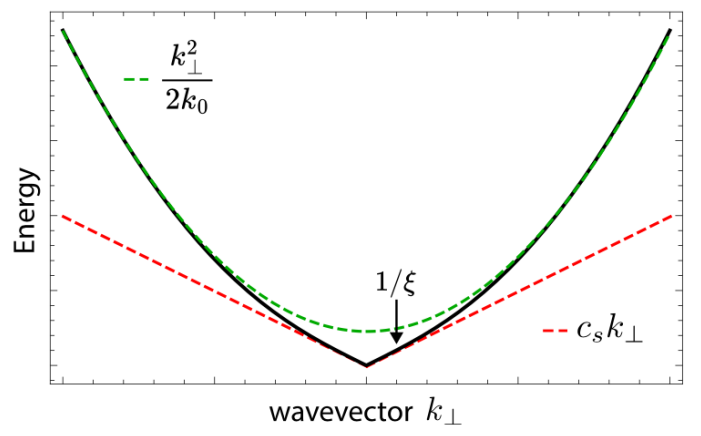
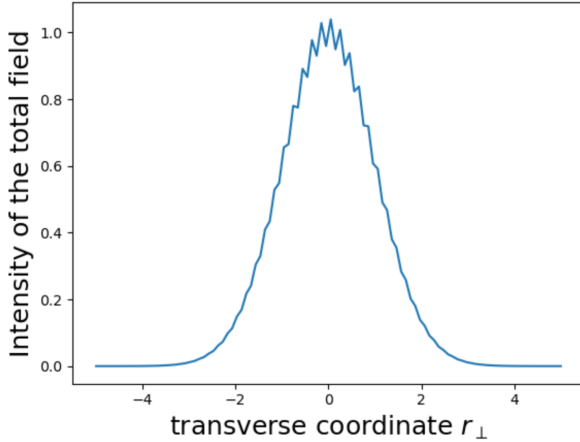


FIGURE 3 – Illustration of a Gaussian mean field and the superimpose fluctuations in arbitrary black. Red is the linear limit at low k_\perp , while green is the large k_\perp with a parabolic shape.

Equation (6) is the **Bogoliubov dispersion**, which is characteristic of weakly interacting Bose gases [13]. This dispersion that we note $\Omega_B(k_\perp)$ shows two regimes plotted in fig.(4) :

- For $k_\perp \ll k_0\sqrt{|\Delta n|}$, the dispersion is linear : $\Omega_B(k_\perp) \approx k_\perp\sqrt{|\Delta n|}$ this is the sonic or phononic regime, which enables us to define a speed of sound $c_s = \sqrt{|\Delta n|}$ in meter per meter.²
- For $k_\perp \gg k_0\sqrt{|\Delta n|}$, we find the dispersion of free massive particules : $\Omega_B(k_\perp) \approx \frac{k_\perp^2}{2k_0}$

To summarize, the **Bogoliubov theory** predicts the behaviour of fluctuations of the electric field envelope in the rubidium cell. These fluctuations can evolve as a phononic wave or as a free massive particle depending on their transverse wave vector k_\perp compared to the inverse of the healing length. These particles will subsequently be called Bogoliubov modes.

2. In BEC field, the sound velocity appears with the standard unity ($m.s^{-1}$) but for fluid of light, the time is the propagation axis

5 How to see a fluid in experiment

To understand the denomination "fluid" of light, it is useful to switch to a hydrodynamic framework. This can be done using Madelung transform, where the field envelope \mathcal{E} is expressed as a function of density ρ and phase ϕ :

$$\mathcal{E}(\mathbf{r}_\perp, z) = \sqrt{\rho(\mathbf{r}_\perp, z)} e^{i\phi(\mathbf{r}_\perp, z)}$$

By injecting this solution in eq(4), it can be shown that we obtain two equations describing the evolution of two hydrodynamic variables (ρ, \mathbf{v}) named quantum Euler equations :

$$\frac{\partial \rho}{\partial z} + \frac{1}{c} \nabla_\perp (\rho \mathbf{v}) = -\alpha \rho$$

$$\frac{\partial \mathbf{v}}{\partial z} + \frac{1}{c} \mathbf{v} \cdot \nabla_\perp \mathbf{v} = c \nabla_\perp \left(\frac{\delta n}{n_0} + \frac{n_2 c \epsilon_0}{2} \rho + \underbrace{\frac{1}{2k_0^2} \frac{\nabla^2 \sqrt{\rho}}{\sqrt{\rho}}}_{\text{Quantum pressure}} \right)$$

Where $\mathbf{v} = \frac{c}{k_0} \nabla_\perp \phi$ is the velocity of the fluid.

The first is a consequence of density conservation (with a loss term) and the second is a convection equation coupling the velocity flow to different source terms on the right-hand side. The last term does not appear in classical hydrodynamic, it is called quantum pressure.

5.1 Off-axis interferometry

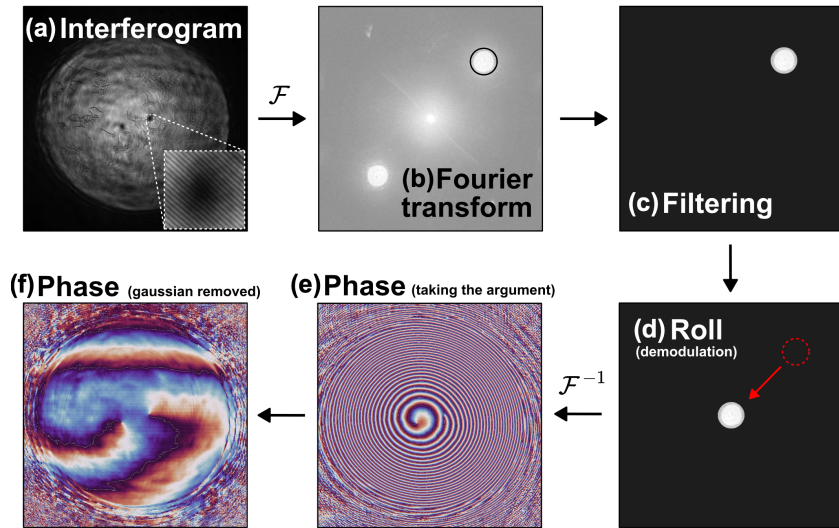


FIGURE 5 – Off-axis interferometry. (a) Intensity measured by a camera. (b) Real part of the 2D Fast Fourier transform. (c) Selection of one of the sidebands. (d) Demodulation to remove the k_\perp component. (e) Argument of the 2D Inverse Fast Fourier transform. (f) Extra-step to flatten the phase, extracted from [14].

A considerable advantage of fluids of light compared to ultracold atomic gases is the simple access to the phase of the field, using interferometric method like off-axis interferometry. The advantage of this method is to collect the phase and amplitude of the field at the same time.

This section is the theoretical description of the experimental set up in the following section 6.2.

The signal beam E_s , which propagated through the non-linear medium, is overlapped with a reference beam E_r . The resulting interference pattern is capture on a camera and can be expressed as follows :

$$\begin{aligned} I_{cam}(\mathbf{r}_\perp) &\propto |E_s(r_\perp)e^{i\phi(\mathbf{r}_\perp)} + E(\mathbf{r}_\perp)e^{ik_r\mathbf{r}_\perp}|^2 \\ &= \underbrace{I_s(\mathbf{r}_\perp) + I_r(\mathbf{r}_\perp)}_{\text{DC part}} + \underbrace{E_s^*E_r e^{-i(\phi-\mathbf{k}_r\mathbf{r}_\perp)} + E_sE_r^* e^{i(\phi-\mathbf{k}_r\mathbf{r}_\perp)}}_{\text{Modulated part}} \end{aligned} \quad (7)$$

Where \mathbf{k}_r is the transverse wave vector of the reference beam with respect to the signal. In order to demodulate the signal and recover $[E_s e^{i\phi}]$, we take the Fourier transform³ of the expression (7).

$$\tilde{I}_{cam}(\mathbf{k}_\perp) \propto \underbrace{\tilde{I}_s(\mathbf{k}_\perp) + \tilde{I}_r(\mathbf{k}_\perp)}_{\text{DC part}} + TF[E_s e^{-i\phi(\mathbf{r}_\perp)}](\mathbf{k}_\perp) \circledast \tilde{E}_r(\mathbf{k}_\perp + \mathbf{k}_r) + TF[E_s e^{i\phi(\mathbf{r}_\perp)}](\mathbf{k}_\perp) \circledast \tilde{E}_r^*(\mathbf{k}_\perp - \mathbf{k}_r)$$

Then the field can be extracted from the sidebands, but the difficulty is that the convolution product is hard to invert. However, if one uses a very large reference beam compared to the signal beam, its Fourier transform will be much narrower than that of the signal. We can then approximate the Fourier transform of the reference using a Dirac function, which means that the convolution product will simply shift the signal by \mathbf{k}_r in the Fourier plane. In this scenario, the camera intensity in the Fourier domain becomes :

$$\tilde{I}_{cam}(\mathbf{k}_\perp) \propto \underbrace{\tilde{I}_s(\mathbf{k}_\perp) + \tilde{I}_r(\mathbf{k}_\perp)}_{\text{DC part}} + \underbrace{TF[E_s e^{-i\phi(\mathbf{r}_\perp)}](\mathbf{k}_\perp - \mathbf{k}_r) + TF[E_s e^{i\phi(\mathbf{r}_\perp)}](\mathbf{k}_\perp + \mathbf{k}_r)}_{\text{modulated part (sidebands)}}$$

We then spatially filter the Fourier plane in order to recover the information carried by the sidebands. This is done with a band-pass filter $\tilde{T}(\mathbf{k}_\perp)$ around one of the first sideband terms, and by shifting the signal in Fourier domain by $-\mathbf{k}_r$ to eliminate the off-axis term. Applying an inverse Fourier transform, we recover :

$$E_s e^{i\phi(\mathbf{r}_\perp)} \circledast TF^{-1}[\tilde{T}](\mathbf{r}_\perp)$$

If the band-pass filter $\tilde{T}(\mathbf{k}_\perp)$ has a circular shape, its inverse Fourier transform, $TF^{-1}[\tilde{T}]$, corresponds to an Airy function. This implies that the recovery process is not perfect as it degrades the spatial resolution of the reconstructed field. We select the largest possible region around the satellite peak in the Fourier plane which still excludes the zeroth order.

6 First steps in the lab

This section aims to explain how to experimentally obtain a fluid of light. It can serve as a guideline to build an experiment for future interns. All of the required engineering is explained in details. I will use the theory in section 3 to enhance light-matter interaction.

3. We will use both $TF[X]$ and \tilde{X} to describe the Fourier transform of X

6.1 Rubidium cell

To start the experiment, you need to find a $\chi^{(3)}$ nonlinear medium. In the lab, we have many cells composed of rubidium atoms of different sizes, shapes and compositions. So, choosing the right cell requires considerations.

The cell can be pure or composed of a mixture of vapor ^{85}Rb and ^{87}Rb . For a mixture, the cell is composed of two isotopes : 72% is ^{85}Rb and 28% of ^{87}Rb . For some application, it can be useful to have a cell with a pure composition but they are more expensive. I chose a cylindrical cell composed of a mixture for easy installation and a cell that was not too long (7.5cm) to avoid suffering excessive absorption.

The aim is to enhance light-matter interactions, to do it we plan to work with warm vapor and address an optical transition of ^{87}Rb with a laser. Since the nonlinear response of the medium depends on the density of the atoms.

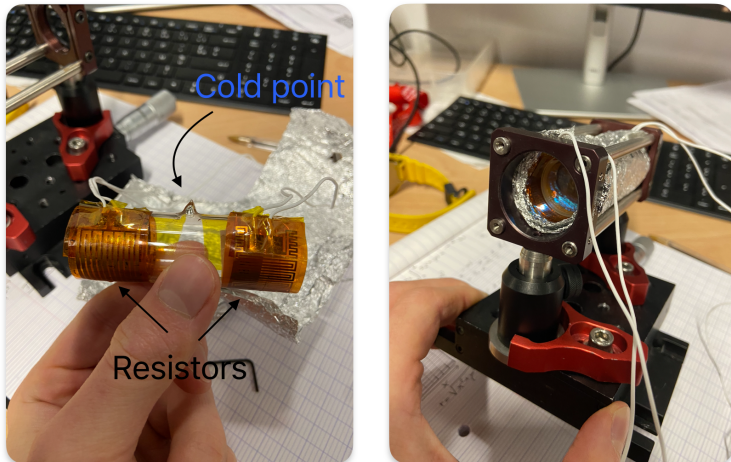


FIGURE 6 – Rb cell and the thermic system. Cold point and two resistors to reduce condensation on the windows. At right the cell wrap in aluminium foil and blocked in a cage.

The first thing to do is to check if you have Rubidium atoms in the cell and if the cell is not damaged. In general, for a cell at room temperature, the gas condenses on the windows. It is necessary to remove it with a heat gun (typical temperature $\approx 200^{\circ}C$) and transport the Rubidium to a cold point. To heat the cell, we use the high-energy dissipation due to Joules effect in a resistor. We connect two resistors of $R = 36,6 \Omega$ in parallel to a power supply that can deliver $U = 15V$ to increase dissipation. Then the power dissipated by this system is $P = \frac{U^2}{R_{eq}} = 12.3W$ with U the voltage and R_{eq} the associated resistor. At the end of the protocol the temperature in the cell can reach $\approx 110^{\circ}C$. Finally, to reduce the thermal radiation, it is necessary to envelop your cell with metal. I prefer to use aluminium foil than copper metal cage. Indeed, for a metal cage, the temperature is more homogeneous but it is more difficult to obtain a high temperature because of the high thermal diffusivity of copper. The aluminium foil is efficient for reflecting infrared radiations and has a low thermal capacity (due to the small volume) that allows the temperature to be increase by injecting less energy.

6.2 Off-axis interferometry experiment

Once the Rb cell is ready, the next step to set up an optical experiment, in particular an interferometer, to measure phase. We have seen in section 5.1 that the off-axis interferometry gives access to amplitude and phase. I will start by presenting the experimental setup.

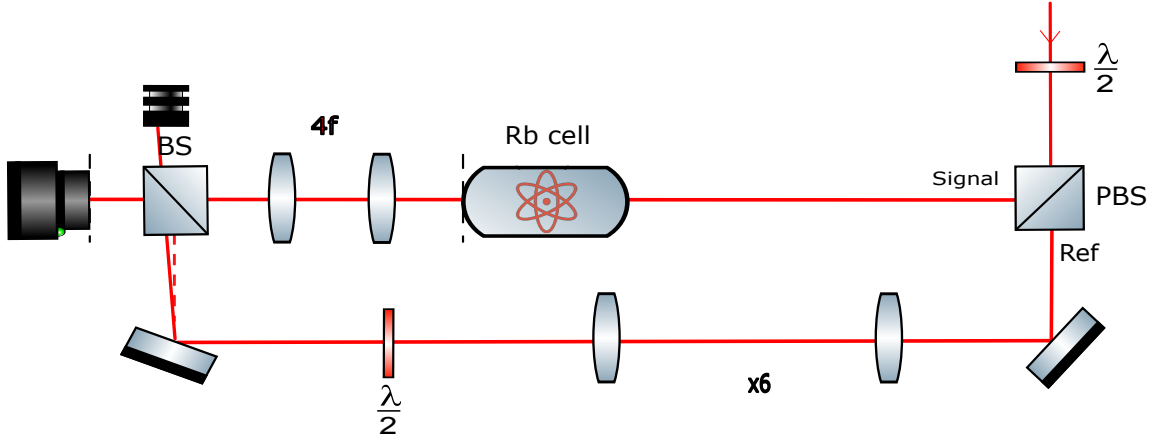


FIGURE 7 – Experimental set up for Off axis interferometry to access the amplitude and phase of the fluid just after the cell. As a Mach-Zehnder interferometer, we split the initial beam in two paths : signal and reference to probe the properties of the Rb cell using the signal beam .

To implement an interferometer, a laser Precilaser (Fixed external cavity) takes the role of a coherent source at 780 nm . The tunable laser allows us to address the D2 transition between hyperfine states ($F=2 \rightarrow F'$) of $^{87}\text{Rb}^4$, to see more detail on this alkali atom [15]. To describe the experimental set up fig.(7), I will follow the path of the light. To start, I place a collimator to obtain a collimated beam at the fiber output. In fact, because of the transverse confinement in the fiber, the beam diverge a lot at the output. I use a Polarized Beam Splitter (PBS) and a wave plate $\frac{\lambda}{2}$ to create and adjust the power of two beams : reference beam and signal (according to the definition section 5.1) After this, the size of the reference beam is increased by a factor 6 compared to the signal with a telescope, a $\frac{\lambda}{2}$ allows to have the same polarization as the signal. I set up now a 4f imaging system to image the output of the cell onto the camera, a beam splitter (BS) allowing one to recombine the signal and the reference. The last thing to do is to play with the rotation screws on the BS and the reference mirror to find the good angles to separate the DC term (at $k_{\perp} = 0$) and the AC term at k_r . With the ideal angles, the signals are well separated in the Fourier space and overlaped in real space, this allows the field to be correctly extracted. Now on the camera, we observe the interferogram fig.5(a) produced by the superposition of the signal and the reference. The diagonal line on the zoom is the interference signal. The data processing to reconstruct the field is illustrated on fig.5 from the interferogram collected by a camera. I have adapted to my camera the initial code created by a previous Ph.D student. This code can be seen in the appendix.

4. A wave meter give a direct access to the central wavelength and the detuning. Since the Doppler effect is important, we address all the transitions in the hyperfine structure of the excited state $F' = \{1, 2, 3\}$

7 Measurement of the nonlinear index

To conclude the development of the off-axis interferometry method, I would like to show a measurement that can be performed with this set-up. I will compute the nonlinear index n_2 by measuring the nonlinear phase shift.

The signal passing through the cell acquires a phase that can be extracted by the off-axis method. This accumulated phase $\Delta\phi$ can be written as the sum of the phase at each evolution step dz in the cell. Since the cell exhibits linear losses, the intensity can be described according to the Beer-Lambert law. Since the field is Gaussian, the intensity distribution depends on the (x,y) coordinates in the transverse plan. Consequently, the accumulated phase depends also on the transverse coordinates due to self phase modulation :

$$\Delta\phi(x, y, L) = k_0 n_2 \int I_0(x, y) e^{-\alpha z} dz + \phi_0$$

with $I_0(x, y)$ the initial transverse laser intensity at $z=0$ at the position (x, y) , L the size of the cell, α the linear losses, ϕ_0 the phase reference between the ref and the signal.

It is hard to determine the phase reference ϕ_0 due to the different paths taken by both beams. To cancel the phase reference, we will investigate the phase accumulated at two different points on the beam, see the red points fig.(8). To do that, we measure the intensity at the top of the Gaussian intensity distribution (corresponding to the point located at (x_{max}, y_{max})) and at the minimum at the bottom (corresponding to the point located at (x_{min}, y_{min})). We also measure the linear losses by measuring power at the input and at the output of the cell.

$$\Delta\phi' = \Delta\phi(x_{max}, y_{max}, L) - \Delta\phi(x_{min}, y_{min}, L) = k_0 n_2 \int (I_0(x_{max}, y_{max}) - I_0(x_{min}, y_{min})) e^{-\alpha z} dz + \phi_0 - \phi_0 \quad (8)$$

We have access to the nonlinear refractive index n_2 by inverting the relation 8 :

$$n_2 = \Delta\phi' \frac{\alpha}{k_0 \Delta I_0} (1 - e^{-\alpha L})^{-1} \quad (9)$$

7.1 Measurement protocol

Following the theoretical expression of n_2 eq.(9), the off-axis interferometry method gives us access to the accumulated phase $\Delta\phi(x, y, L)$. Thanks to this, we can compute the phase difference between the minimum and the maximum denoted $\Delta\phi'$. Also, we measure the output intensity at the center of the Gaussian beam with a camera. We also measure linear losses α due to absorption by measuring the power at the input and the output of the cell using a powermeter.

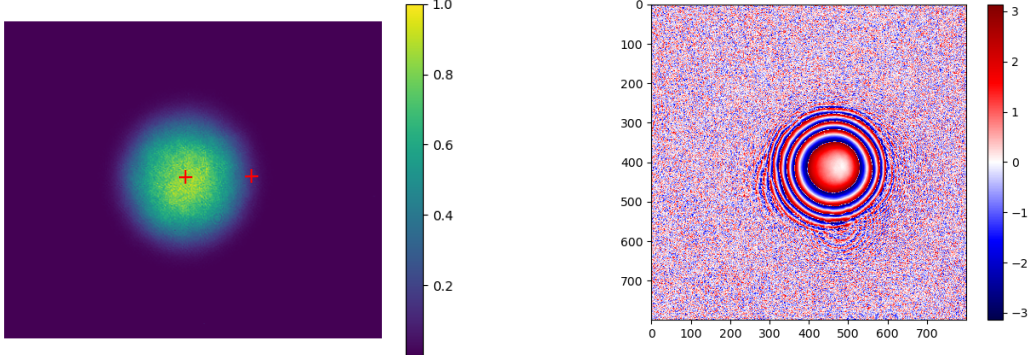


FIGURE 8 – Normalized Intensity distribution in the transverse plan, the red points corresponds to maximum (central point) and minimum of intensity.

FIGURE 9 – The phase of the field at the output of the Rb cell, obtain using off-axis interferometry method, all the values are contains between $-\pi, \pi$

7.2 Analysis protocol

Once these images are collected, they are analysed in Python to extract the phase⁵. Since the phase is 2π -periodic, it is necessary to unwrap the phase to know the accumulated phase depending on (x, y) . To reduce the uncertainty, we performed an azimuthal average. After this, we need to measure the phase difference between the maximum intensity and the minimum intensity.

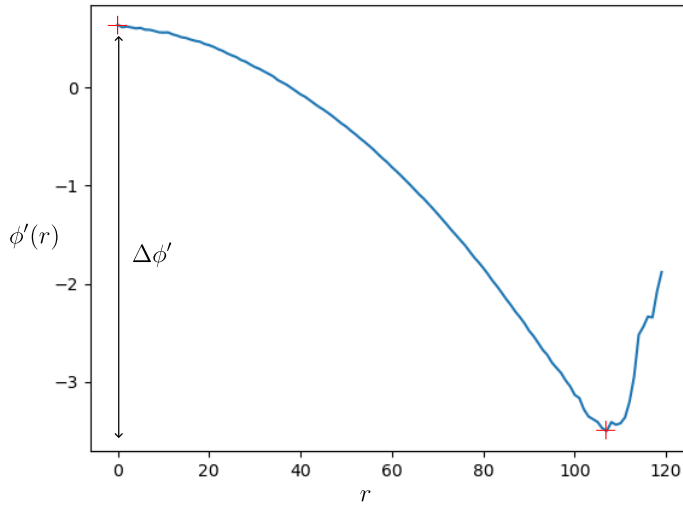


FIGURE 10 – Azimuthal average of the unwrap phase, which correct the periodic discontinuity. The accumulated phase $\Delta\phi$ is represented with a narrow.

This unpacking phase measure gives us access to the local phase difference $\Delta\phi'$. After this we perform a measurement of the linear absorption coefficient, which depends on the ratio between the output and input intensity according to the Beer-Lambert law. This cell of length $L = 1 \text{ cm}$, the detunning is $\delta \approx -1 \text{ GHz}$, under experimental conditions produces a nonlinear index of refraction :

$$n_2 = -1,93 \cdot 10^{-9} \text{ m}^2 \cdot \text{W}^{-1}$$

5. All the Python codes created during this internship are in the appendix

8 Quantum effects

In this section, I get to the heart of the subject of my internship. All the previous sections operate within a classical mean-field regime, described accurately by the Gross-Pitaevskii equation. Now we will investigate quantum fluctuations and correlations in a paraxial fluid of light. Quantum depletion is a BEC phenomenon in which a fraction of the condensate is pumped out of the condensate because of interactions. We will investigate the analogous phenomenon of quantum depletion for a fluid of light. We will develop and present the best observable for observing this effect and how to measure it.

8.1 Beyond mean-field

With a quantum point of view, light is quantized, the electric field becomes an operator, and the measured field is the eigenvalue of this operator for a certain state. The free field quantization can be understood as a sum over all modes that can exist, since we are not in a box, it is a continuous sum. Then an electric field can be decomposed with the positive (+) and negative (-) frequencies [16] :

$$\hat{E}(\mathbf{r}, t) = \hat{E}^{(+)}(\mathbf{r}, t) + \hat{E}^{(-)}(\mathbf{r}, t)$$

$$\hat{E}^{(+)}(\mathbf{r}, t) = i \int \sqrt{\frac{\hbar\omega(\mathbf{k})}{2\epsilon_0}} \hat{a}(\mathbf{k}) e^{i(\mathbf{k}\cdot\mathbf{r}-\omega(\mathbf{k})t)} \frac{d\mathbf{k}}{(2\pi)^3}$$

The envelope for a monochromatic beam can be written simply as, by putting all the constant in \hat{a} :

$$\hat{\mathcal{E}}(\mathbf{r}_\perp, z) = \int \hat{a}(\mathbf{k}_\perp) e^{-i\mathbf{k}_\perp \cdot \mathbf{r}_\perp} d\mathbf{k}_\perp \quad (10)$$

With $\hat{a}(k)$ the annihilation operator and $\sqrt{\frac{\hbar\omega(\mathbf{k})}{2\epsilon_0}}$ is the photon amplitude of a mode with k wave vector. The laser in the paraxial regime can be seen as a spatially coherent plane wave where the number of photons is concentrated in a Dirac peak at $k_\perp = 0$ (see the initial state in blue, fig.(12))

8.2 Four-wave-mixing process

To fully understand the fundamental impact of vacuum in the generation of correlated pairs. We will interpret the non-linear interaction in the medium as a four-waves mixing process.

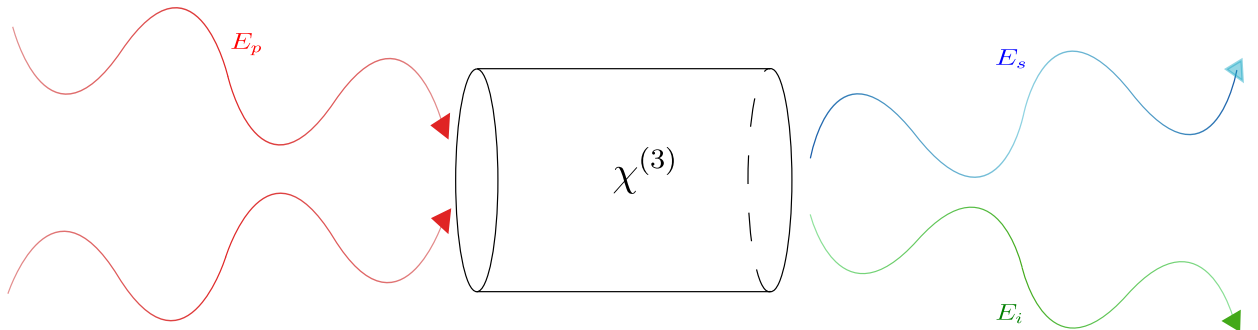


FIGURE 11 – Scenario of Four wave mixing process. 2 input channels at left are taken by an intense pump field E_p and 2 output channels represent the signal E_s and idler E_i

We consider four waves in a $\chi^{(3)}$ medium. The input field is called the pump fields E_p , the fields

at the output are signal E_s and idler E_i . To have an efficient process, the waves must respect phase matching relations :

$$2\omega_p = \omega_s + \omega_i$$

$$2\vec{k}_p = \vec{k}_3 + \vec{k}_4$$

Considering classical field for the input fields, the interacting Hamiltonian of the system can be written in a easy manner :

$$\hat{H}_{int} = \epsilon \hat{a}_s^\dagger \hat{a}_i^\dagger + \epsilon^* \hat{a}_s \hat{a}_i$$

Where ϵ is a interaction coefficient that depend of the pump intensity and the nonlinear properties of the medium. \hat{a}_s/\hat{a}_i is the annihilation operator in signal/idler mode.

The initial quantum state is vacuum for the signal and idler mode :

$$|\psi(0)\rangle = |0_s\rangle \otimes |0_i\rangle$$

After a time evolution, the state becomes :

$$|\psi(t)\rangle = e^{-\frac{i\hat{H}_{int}t}{\hbar}} |\psi(0)\rangle$$

A first order Taylor expansion give us :

$$|\psi(t)\rangle \approx |0\rangle + c_1 |1_s, 1_i\rangle$$

The development show that even starting with vacuum mode in the signal and idler mode the system can generated a correlated photons pairs $|1_s, 1_i\rangle$. In this case, we talk about spontaneous-four-waves mixing, since this random event occurs thanks to vacuum fluctuations.

8.3 Input-output approach

The Rb cell and the different processes concerning the photon/Bogoliubov mode can be studied using the input-output approach.

The physical situation represented in fig.(12) is the following : The initial state before $z=0$ is a spatially coherent state, where all photons have the same wave vector $\mathbf{k}_\perp = 0$ that evolve freely⁶. In quantum optical language, all the modes except $\mathbf{k}_\perp = 0$, which contain a macroscopic number of photons, are vacuum modes. To keep an intuition about that, it is useful to do the mapping with the BEC language. The initial state, where all the photons have the same wave vector, is **analogous to a BEC** where all particles have zero momentum. The photon gas enters the cell and the interaction strength g is suddenly non-zero (the interactions are quenched). A way to adress this problem is to consider that the interacting photons are quasiparticles without interaction and evolve harmonically following Bogoliubov dispersion. Outside the cell, for $z < 0$ and $z > L$ the interaction strength is zero.

Inside the medium, the photon gas adopts a collective behaviour, $\hat{b}_{\mathbf{k}_\perp}$ describes a **Bogoliubov quasi-particle** which represents a photon at k_\perp in the cell that interacts with its environment. So by doing

6. Outside the medium, without interactions and potential field, the evolution of photons is only guided by diffraction.

a change of basis (11) at each cell surface and by diagonalizing the Hamiltonian of the system⁷, the Bogoliubov mode appears as the eigenmode of the photon gas in interaction.

$$\begin{pmatrix} \hat{a}_{\mathbf{k}}(z) \\ \hat{a}_{-\mathbf{k}}^\dagger(z) \end{pmatrix} = \underbrace{\begin{pmatrix} u_{\mathbf{k}}(z) & v_{\mathbf{k}}(z) \\ v_{\mathbf{k}}(z) & u_{\mathbf{k}}(z) \end{pmatrix}}_{\mathcal{B}_{\mathbf{k}}} \begin{pmatrix} \hat{b}_{\mathbf{k}}(z) \\ \hat{b}_{-\mathbf{k}}^\dagger(z) \end{pmatrix} \quad (11)$$

Where $\mathcal{B}_{\mathbf{k}}$ is an hyperbolic rotation : $u_{\mathbf{k}}^2 - v_{\mathbf{k}}^2 = 1$ that allows us to include the photon-photon interaction. Its spectrum is the **Bogoliubov dispersion** presented section in 4.

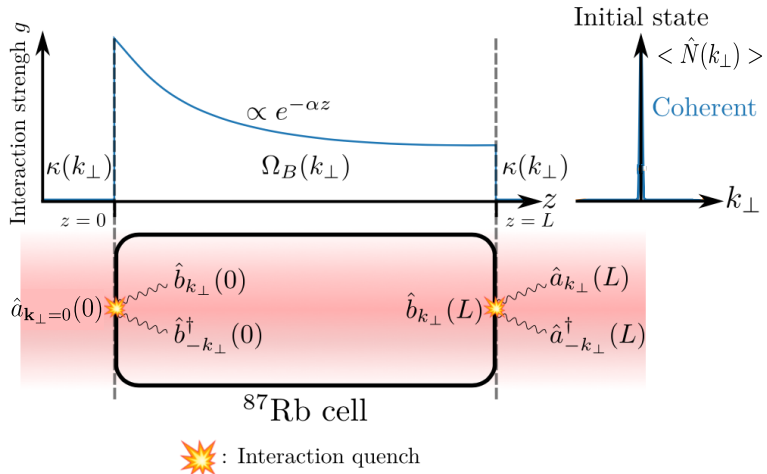


FIGURE 12 – The cell is represented and the creation of pairs of Bogoliubov mode (resp. photons) is highlighted at the input and output of the cell with the orange symbols. The strength of the interaction profile is represented in parallel above the cell : within the cell the interaction strength decreases exponentially due to absorption, and the interactions are abruptly switched on and off at the input and output of the cell. The initial state represent the initial population distribution, extracted from [12]

The quench, this event that suddenly turns on and off of the interaction generated a **highly correlated pairs of Bogoliubov modes** ($\hat{b}_{\mathbf{k}}, \hat{b}_{-\mathbf{k}}$). In the optical language, this process of emission of photon pairs at wave vectors (and/or frequencies) different from the incident ones goes under the name of spontaneous four-wave mixing. [17] After the propagation in the cell, the correlation is conserved and can theoretically be obtained by making a measurement of the **population operator in reciprocal space** $\hat{N}(\mathbf{k}_\perp)$. This observable represents the number of photons that get out of the condensate/the initial mode. For a BEC, this quantity corresponds to the number of Bosons that gained momentum due to interactions. The spontaneous-four-mixing that depopulates the initial $\mathbf{k}_\perp = 0$ mode due to vacuum fluctuations then appears to be a phenomenon analogous to quantum depletion in a BEC.

7. It is hamiltonian can be seen in [17], but it is omitted because it is not central to the discussion

9 Theoretical description of correlations in momentum space

In this section, I will develop the prediction of the spontaneous four-wave mixing that is presented in [17]. Then, the section outlines our investigation on this topic.

9.1 Theoretical description of the spontaneous-four-wave mixing

The quench induces a wave vector redistribution and correlation between the particles. Due to interaction, a certain number of photons initially at $\mathbf{k}_\perp = 0$ will obtain a transverse wave vector. The quantity of interest that quantify this process is the mean value of the **population operator** $\langle \hat{N}(\mathbf{k}_\perp) \rangle$. With a quantum optical language, this quantity corresponds to the spontaneous-four-wave-mixing intensity distribution fig.13. To understand this denomination, it will be useful to decompose a four-wave mixing event at an interface for two photons. Considering the first interface : initially, two photons in the mode $\mathbf{k}_\perp = 0$ arrives at the interface, at the output the signal and idler are vacuum mode. These incident photons suddenly acquires a huge amount of energy, the only way it can dissipate energy is to generate the correlated pairs. Then, the quench of interaction produces a correlated pair (signal and idler) from vacuum mode $\mathbf{k}_\perp \neq 0$. Since the mean value of the number of photons in all vacuum modes ($\hat{a}(\mathbf{k}_\perp \neq 0)$) is zero, it is actually the vacuum fluctuations that seed the emission of the Bogoliubov modes. The most noticeable feature of the momentum distribution is its oscillation profile which originates from $\mathbf{k}_\perp = 0$. Depending on the value of the wave vector \mathbf{k}_\perp , the two-body emission processes at the front and back interfaces reveal constructive or destructive interferences at well-defined periods. The analytical formula for the mean value of the population operator is the following :

$$\langle \hat{N}(\mathbf{k}_\perp) \rangle = A \ell^2 \operatorname{sinc}^2\left(\frac{\ell}{2} \kappa \sqrt{\kappa^2 + 4}\right) \quad (12)$$

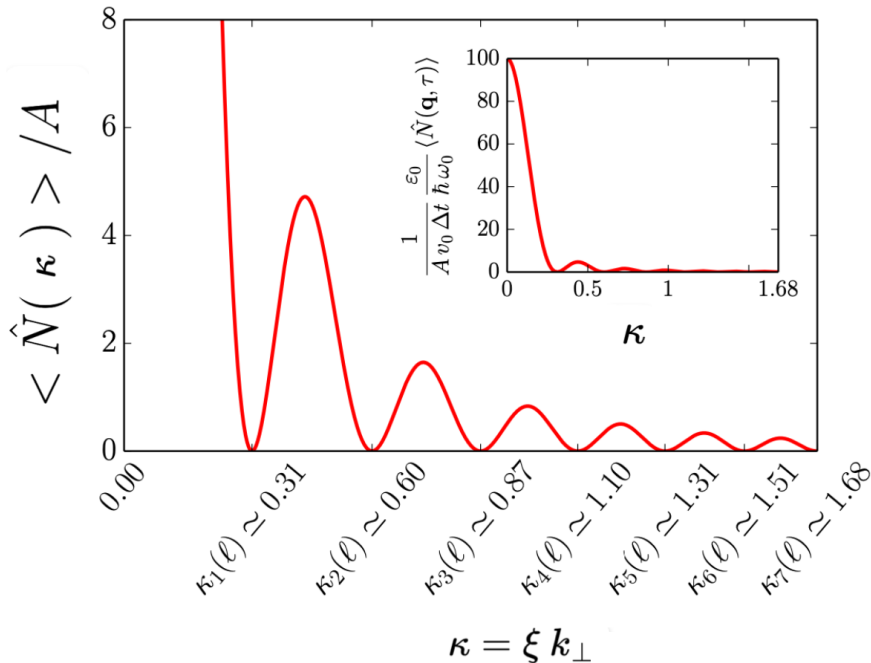


FIGURE 13 – Momentum distribution,(equation (12)) The main plot focuses on the oscillations of the momentum distribution while the inset shows the whole function. Adapted from [17].

With $\ell = k_0 \Delta n L$ which corresponds to the strength interaction parameter and $\kappa = \xi |\mathbf{k}_\perp|$ dimensionless quantities with all other physical quantities already presented in section 3.2. For simplicity, we have set A as a normalized constant.

There exists some transverse wave vector for which the quasi-particle interferes destructively at this end of the cell. These events correspond to the zero minima in the momentum distribution. This typical periodic value labelled $\kappa_n(\ell)$ follows the law :

$$k_n(\ell) = \sqrt{2} \sqrt{\sqrt{\left(\frac{n\pi}{\ell}\right)^2 + 1} - 1}$$

Where n in an integer ≥ 1

9.2 Correlation in far-field regime

Having access to $\hat{N}(\mathbf{k}_\perp)$, it can be possible to see the quantum nature of the emitted particles via a measurement of the two-point correlation function in the far-field regime, namely :

$$g^{(2)}(\mathbf{k}_\perp, \mathbf{k}'_\perp) = \frac{\langle \hat{N}(\mathbf{k}_\perp) \hat{N}(\mathbf{k}'_\perp) \rangle}{\langle \hat{N}(\mathbf{k}_\perp) \rangle \langle \hat{N}(\mathbf{k}'_\perp) \rangle} \quad (13)$$

This is a function which quantifies the correlations between the different angular components of the four-wave mixing emission. A long mathematical development permits us to show that the correlation function $g^{(2)}$ takes a simple form [17] :

$$g^{(2)}(\mathbf{k}_\perp, \mathbf{k}'_\perp) = \gamma(\mathbf{k}_\perp, \mathbf{k}'_\perp) [\delta(\mathbf{k}_\perp - \mathbf{k}'_\perp) + \delta(\mathbf{k}_\perp + \mathbf{k}'_\perp)]$$

The **two-body correlation** signals in reciprocal space must be concentrated along the diagonal $(\mathbf{k}_\perp, \mathbf{k}'_\perp) = \mathbf{k}_\perp$ and antidiagonal $(\mathbf{k}_\perp, \mathbf{k}'_\perp) = -\mathbf{k}_\perp$ lines. The first one reflects the vacuum fluctuations in the occupation $\hat{N}(\mathbf{k}_\perp)$ since the initial state is a coherent plane wave where the number of photons is a Dirac peak in $\mathbf{k}_\perp = 0$. The second is a clear signature of a complete correlation between excitations of opposite wave vectors $\pm \mathbf{k}_\perp$. To correctly interpret the significance of this correlation function, this function compares the number of particles according to their transverse wave vector.

In summary, the quench produces a pair of correlated particles in the wave vector. To quantify this number, we will use the observable $\hat{N}(\mathbf{k}_\perp)$. The mean value of this observable has an oscillating behaviour due to the interference between the correlated pair. The quantum nature of these particles can be highlighted using $g^{(2)}$, a correlation function that compares the number of particles in two given directions.

9.3 A good observable $\hat{N}(\mathbf{k}_\perp)$

The first step to study the quantum aspect of the fluid of light is to understand the theory presented section 9.1 and 9.2. We understood that $\hat{N}(\mathbf{k}_\perp)$ is the product of the Fourier transform of the total field $\hat{\mathcal{E}}$ and its conjugate⁸. The oscillating behaviour of $\hat{N}(\mathbf{k}_\perp)$ is encapsulated in the second order of field fluctuations. In fact, we can do a mode decomposition (in terms of wave vector) of the annihilation operator \hat{a} ⁹. $\hat{N}(\mathbf{k}_\perp)$ appears as a sum of a macroscopic number of particles N_0 in $\mathbf{k}_\perp = 0$ that corresponds to the spatially monochromatic classical plane wave and a second order in fluctuation $\delta\hat{a}(\mathbf{k}_\perp)^\dagger\delta\hat{a}(\mathbf{k}_\perp)$.¹⁰

$$\langle \hat{N}(\mathbf{k}_\perp) \rangle = N_0\delta(\mathbf{k}_\perp) + \langle \delta\hat{a}(\mathbf{k}_\perp)^\dagger\delta\hat{a}(\mathbf{k}_\perp) \rangle$$

With this approach, $\delta\hat{a}$ is the part of the field where $\mathbf{k}_\perp \neq 0$. Since the initial state is composed of vacuum modes for all $\mathbf{k}_\perp \neq 0$ except $\mathbf{k}_\perp = 0$ that contain a macroscopic number of particles. $\delta\hat{a}$ comes from the fluctuations of vacuum modes. So, the oscillation behaviour of the number operator comes from the second order in fluctuation.

Now, we understand what $\hat{N}(\mathbf{k}_\perp)$ physically means , the next question is how we can have access to this quantity.

9.4 Measurement protocol

This section is an implementation of the previous theoretical section. I will present the protocol to obtain a measurement of $\langle \hat{N}(\mathbf{k}_\perp) \rangle$.

We have seen that $\langle \hat{N}(\mathbf{k}_\perp) \rangle$ is linked to the Fourier transform of the field. So, the first step is to recover the total field (amplitude and phase) just after the cell using off-axis interferometry (section 5.1) with the 4f imaging system presented in the first experiment 6.2. After this, we can numerically compute the spatial Fourier transform of the field, this step gives us $\hat{a}(\mathbf{k}_\perp)$ and we have directly we have access to $\hat{N}(\mathbf{k}_\perp)$. It is then necessary to repeat the same measurement and compute the mean value to obtain $\langle \hat{N}(\mathbf{k}_\perp) \rangle$. We have also seen that $\hat{N}(\mathbf{k}_\perp)$ was related to the fluctuation, so it can be computed not taking the entire field but only its fluctuations.¹¹ The final step to highlight the quantum nature of the phenomenon is to compute the correlation function in Fourier space $g^{(2)}(\mathbf{k}_\perp, \mathbf{k}'_\perp)$ and see if we have the two diagonals as predicted by the theory (Section 9.2).

9.5 Experimental set-up to probe the population

Here we present the more advanced set-up that we established. In the same spirit as the measurement of n_2 , we build an interferometer to recover the field after the cell.

8. A discussion in appendix, highlight the subtlety of this observable

9. $\hat{a} = a_0 + \delta\hat{a}$ with $\langle \hat{a} \rangle = a_0$

10. An important point concerning the comparison with the mean-field theory presented section (4) is $\delta\hat{a}$ comes from a quantum effect only, and $\langle \delta\hat{a} \rangle = 0$.

11. Just by a numerical treatment where at each image we remove the mean value

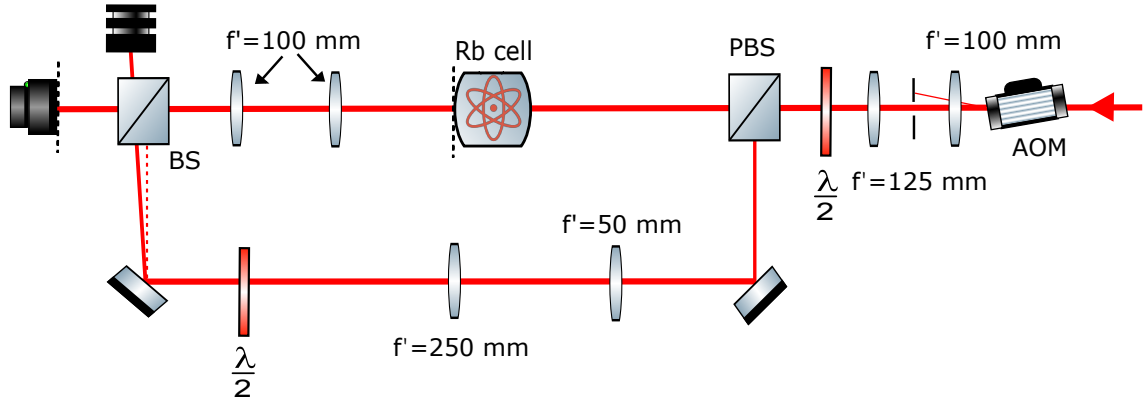


FIGURE 14 – Experimental set-up to measure population operator

We add to the previous set-up an Acousto-optic modulator (AOM) to modulate the intensity of the beam. Thanks to this system we create a pulsed beam in the order 1, the 0 order is filter with a pinhole. This system permits us to increase the intensity of the laser without saturating the camera. The optical system composed of the first lens $f' = 100 \text{ mm}$ and the second lens $f' = 125 \text{ mm}$ is not a confocal system, the distance between both is chosen to correct the phase induced by the AOM. Indeed, we want to have a flat wave front at the input of the cell. Here we have a cell with a lenght of 1 cm composed of a Rb mixture.

9.6 Analysis protocol

To compute the average value of the population operator in Fourier space. We took 200 images of the interferogram. We recover the field for each shot using off-axis interferometry method section 5.1. We compute the spatial Fourier transform of each recovery field. Since we have only plane wave on a small surface, we compute $\frac{\hat{\mathcal{E}}}{\langle \hat{\mathcal{E}} \rangle} = 1 + \frac{\delta \hat{\mathcal{E}}}{\langle \hat{\mathcal{E}} \rangle}$ ¹², to mimic plane wave in average. We compute the population operator $N(\mathbf{k}_\perp)$ of this quantity and do the statistical average on all shots. Ultimately, we then take a slice through the centre and fit these data with the eq.(12) with two parameters (ℓ, κ) .

9.7 Preliminary results and perspectives

In this section, I present the first preliminary result related to the population operator number.

The results fig.(15) demonstrate the measurement detained by following the measurement protocol and analysis presented sections (9.4). It is worth noting that the results appear promising. The fitted function follow the trend of the experimental curve, with the position of the oscillations coinciding. And the vertical symmetry around $\mathbf{k}_\perp = 0$ allows us to believe in the generation of correlated pairs. However, the measurement in the current experiment is limited by the spatial resolution of the camera and the weak nonlinear interaction in the cell. The next step will be to correct these issues by changing a lens in the 4f imaging system to increase the size of the beam and thus increase the spatial resolution. To increase the nonlinear interaction, we will increase the temperature of the cell by changing the heating system.

12. We can write : $\hat{\mathcal{E}} = \langle \hat{\mathcal{E}} \rangle + \delta \hat{\mathcal{E}}$, with $\langle \delta \hat{\mathcal{E}} \rangle = 0$

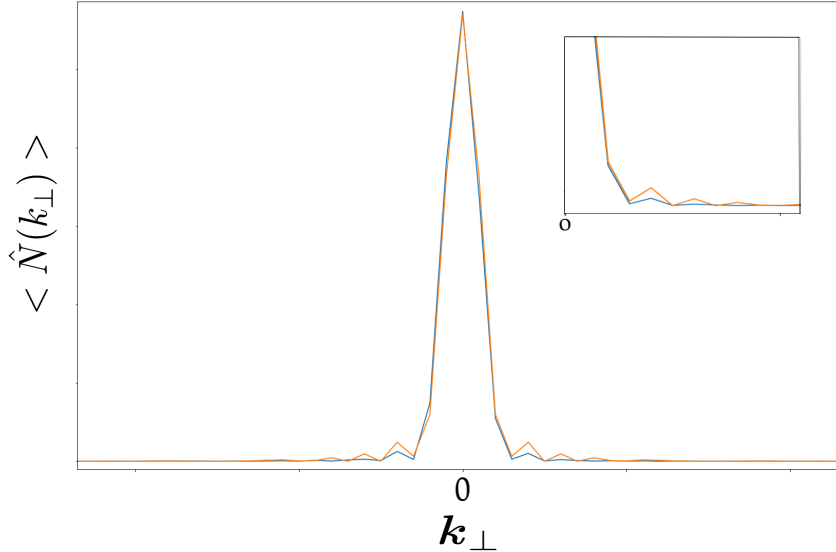


FIGURE 15 – Spontaneous-four-wave mixing, The main plot focuses on the whole function, experimental data in blue and the curve fit according to the eq(12) in orange. The inset shows focus on the oscillations of the moment distribution

After this, we hope to achieve better agreement with the theory. When the fit is suitable with more resolution, we will be able to calculate $g^{(2)}$ and conclude on the existence of a correlation between the Bogoliubov modes and the quantum nature of our system.

10 Conclusion

During this report, we have presented the interest of fluid of light in paraxial regime. We have seen that a pure analogy with the physics of cold atoms is possible and that general phenomena are described by Bogoliubov's theory. After that, we presented the most useful experimental technique : off-axis interferometry, which allows for the recovery of the complete field. We have used this technique to characterise the nonlinear interaction in the rubidium warm vapor. This base allows us to investigate the quantum and correlation effects in a quantum fluid of light. A quantum optics approach of the system led us to describe our system with operator and vacuum mode. We have seen that taking in account the vacuum fluctuation in the nonlinear processes (spontaneous-four-wave mixing) induces pairs correlation. Finally, we present preliminary results related to a measurement of $\langle \hat{N}(\mathbf{k}_\perp) \rangle$ that quantify this process.

Références

- [1] Franco Dalfovo, Stefano Giorgini, Lev P Pitaevskii, and Sandro Stringari. Theory of bose-einstein condensation in trapped gases. *Reviews of modern physics*, 71(3) :463, 1999.
- [2] Vladimir E Zakharov et al. Collapse of langmuir waves. *Sov. Phys. JETP*, 35(5) :908–914, 1972.
- [3] Yuri S Kivshar and Govind P Agrawal. *Optical solitons : from fibers to photonic crystals*. Academic press, 2003.
- [4] Gerald Beresford Whitham. *Linear and nonlinear waves*. John Wiley & Sons, 2011.
- [5] Akira Hasegawa and Frederick Tappert. Transmission of stationary nonlinear optical pulses in dispersive dielectric fibers. i. anomalous dispersion. *Applied Physics Letters*, 23(3) :142–144, 1973.
- [6] Iacopo Carusotto. Superfluid light in bulk nonlinear media. *Proceedings of the Royal Society A : Mathematical, Physical and Engineering Sciences*, 470(2169) :20140320, 2014.
- [7] Lev P Pitaevskii. Vortex lines in an imperfect bose gas. *Sov. Phys. JETP*, 13(2) :451–454, 1961.
- [8] Myrann Baker-Rasooli, Tangui Aladjidi, Nils A Krause, Ashton S Bradley, and Quentin Glorieux. Observation of jones-roberts solitons in a paraxial quantum fluid of ligh. *arXiv preprint arXiv* :2501.08383, 2025.
- [9] Quentin Fontaine, Pierre-Élie Larré, Giovanni Lerario, Tom Bienaimé, Simon Pigeon, Daniele Facio, Iacopo Carusotto, Élisabeth Giacobino, Alberto Bramati, and Quentin Glorieux. Interferences between bogoliubov excitations in superfluids of light. *Physical Review Research*, 2(4) :043297, 2020.
- [10] Myrann Baker-Rasooli, Wei Liu, Tangui Aladjidi, Alberto Bramati, and Quentin Glorieux. Turbulent dynamics in a two-dimensional paraxial fluid of light. *Physical Review A*, 108(6) :063512, 2023.
- [11] Alberto Amo, Jérôme Lefrère, Simon Pigeon, Claire Adrados, Cristiano Ciuti, Iacopo Carusotto, Romuald Houdré, Elisabeth Giacobino, and Alberto Bramati. Superfluidity of polaritons in semiconductor microcavities. *Nature Physics*, 5(11) :805–810, 2009.
- [12] Tangui Aladjidi. *Full optical control of quantum fluids of light in hot atomic vapors*. PhD thesis, Sorbonne Université, 2023.
- [13] Lev Pitaevskii and Sandro Stringari. *Bose-Einstein condensation and superfluidity*, volume 164. Oxford University Press, 2016.
- [14] Quentin Glorieux, Clara Piekarski, Quentin Schibler, Tangui Aladjidi, and Myrann Baker-Rasooli. Paraxial fluids of light. *arXiv preprint arXiv* :2504.06262, 2025.
- [15] Daniel A Steck. Rubidium 87 d line data. 2001.
- [16] A Aiello and JP Woerdman. Exact quantization of a paraxial electromagnetic field. *Physical Review A—Atomic, Molecular, and Optical Physics*, 72(6) :060101, 2005.

- [17] Pierre-Élie Larré and Iacopo Carusotto. Propagation of a quantum fluid of light in a cavityless nonlinear optical medium : General theory and response to quantum quenches. *Physical Review A*, 92(4) :043802, 2015.

Appendix

A Discussion about the observable $\hat{N}(\mathbf{k}_\perp)$

I want to highlight some details on $\hat{N}(\mathbf{k}_\perp)$ and what is observable. This section is optional.

In the literature, the **population operator in the reciprocal space** in this paper is simply written as :

$$\hat{N}(\mathbf{k}_\perp) = \hat{a}^\dagger(\mathbf{k}_\perp)\hat{a}(\mathbf{k}_\perp)$$

but this expression can be very confusing because $\hat{N}(\mathbf{k}_\perp)$ is not the Fourier transform of the population number in position. Moreover, the notation of the conjugate operator in the Fourier space is ambiguous. In fact, by using the quantum formalism introduce in section 8.1 we can define the Fourier transform of the annihilation operator/field as :

$$TF_{\mathbf{k}_\perp}[\hat{a}(\mathbf{r}_\perp)] = \int \hat{a}(\mathbf{k}_\perp)e^{-i\mathbf{k}_\perp \cdot \mathbf{r}} d\mathbf{r}$$

But $\hat{a}^\dagger(\mathbf{k}_\perp)$ is not the Fourier transform of $\hat{a}^\dagger(\mathbf{r}_\perp)$.

Taking this into account, the correct expression of $\hat{N}(\mathbf{k}_\perp)$ as

$$\hat{N}(\mathbf{k}_\perp) = (\hat{a}(\mathbf{k}_\perp))^\dagger \hat{a}(\mathbf{k}_\perp)$$

In this situation the operator is an observable. The thought to keep in mind is that the Fourier transform of the conjugate is not the conjugate of the Fourier transform. The operator "takes the Fourier transform" and conjugate does not commute.

B Quantum physic in experiment

This section aims to highlight an abstract idea/object in quantum mechanics. It presents and lists some thoughts on abstract objects in this field.

B.1 Mean value of an observable

Eigenvalue and observable : Consider an observable \hat{O} . In a course of quantum mechanics, the quantities of interest are the eigenvalue and the eigenstate of this operator that correspond to the possible value that can take this operator for an accessible state. Mathematically, considering an eigenstate $|\phi\rangle$ the eigenvalue is given by the mean value of this operator $\langle\phi|\hat{O}|\phi\rangle$. But how do we experimentally access this value, and what is the significance of this average for an abstract state ?

To illustrate this thought, we take an example in which the observable is the intensity measured by a camera. We write \hat{i} an operator that measures the intensity. The laser field properties are encapsulated in the coherent state. Thus, making a measurement of $\langle\hat{i}\rangle$ corresponds to physically making $N \gg 1$ measurements of the intensity and taking the **statistical average**. Fluctuations are accessible by removing the mean value. Now we have better intuition on this notation $\hat{i} = \langle\hat{i}\rangle + \delta\hat{i}$, so physically \hat{i} is a measurement of a single shot on a camera.

B.2 Statistical approach of correlations

Since the mean value of an observable is a statistical average. We can interpret observables as **random variables**.

$$g^{(2)}(\tau) = \frac{\langle \hat{I}(t)\hat{I}(t+\tau) \rangle}{\langle \hat{I}(t) \rangle \langle \hat{I}(t+\tau) \rangle}$$

According to the statistical approach $I(t)$ and $I(t+\tau)$ are random variables. The autocorrelation function can be written using the probability tools :

$$g^{(2)}(\tau) = \frac{\text{Cov}[I(t), I(t+\tau)]}{E(I(t))E(I(t+\tau))} + 1$$

Where $E(X)$ is the expected value of the random variable X and $\text{Cov}[X, Y]$ is the covariance of X, Y .¹³

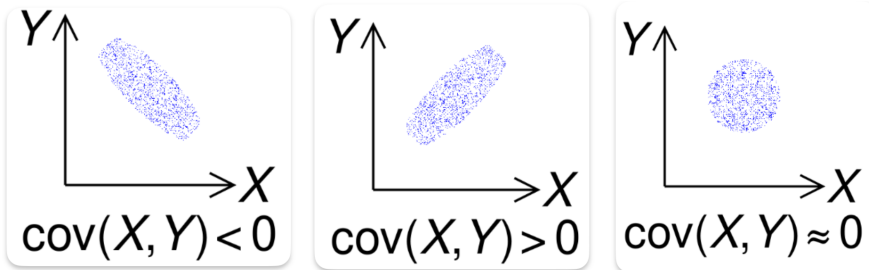


FIGURE 16 – Sketch of covariance according the relation between two random variables X,Y

A measurement of $g^{(2)}$ corresponds to measure the covariance between two random variables. The fig.16 present 3 distinct behaviours. Written intensity as : $I(t) = \mathcal{E}^\dagger(t)\mathcal{E}(t)$. The expression of $g^{(2)}$ with a quantum approach must be in the normal ordering :

$$g^{(2)}(\tau) = \frac{\langle \hat{\mathcal{E}}^\dagger(t)\hat{\mathcal{E}}^\dagger(t+\tau)\hat{\mathcal{E}}(t)\hat{\mathcal{E}}(t+\tau) \rangle}{\langle \hat{I}(t) \rangle \langle \hat{I}(t+\tau) \rangle}$$

In particular, most of the time the autocorrelation function is used to show the quantum aspect of light. At this particular time delay $\tau = 0$, the operator doesn't commute if the modes are not spatially space.

It is necessary to respect time depend commutation relation :

$$[\hat{\mathcal{E}}(t), \hat{\mathcal{E}}^\dagger(t')] = \delta(t-t')$$

The quantum statistical properties of light then follow from the existence of this commutation relation.

13. $\text{Cov}[X, Y] = E[XY] - E[X]E[Y]$

C Python codes

```
Modules to import
[ ]: module to import:import numpy as np
      import matplotlib.pyplot as plt
      from skimage.restoration import unwrap_phase
      from scipy import ndimage
      from scipy import constants

off axis code to recover the field after the cell using a interferogram
[ ]: def off_axis(frame):
      TF_frame=np.fft.rfft2(frame)

      i,j=TF_frame.shape
      radius=j*( np.sqrt(17) - 1 ) / 8
      center=(i/2,j-radius)

      x,y=np.indices(TF_frame.shape)
      TF_frame[(y-center[1])**2+(x-center[0])**2>radius**2]=0           #mask
      TF_frame=TF_frame[i//2+int(radius) : i//2+int(radius),j-int(2*radius) : j]           #translation in k space
      field=np.fft.ifft2(np.fft.ifftshift(TF_frame))
      field=field*np.exp(-1j*np.angle(field[int(barycentre(field)[0])][int(barycentre(field)[1])])) #to compensate the phase shift at each shoot

      return field
```

with the off-axis code we can direclty extract : the **amplitude** of the field with `np.abs(off_axis(frame))**2` and the **phase** with : `np.angle(off_axis(frame))`

```
To compute the barycenter from an image, using the definition  $\frac{\int f(x,y) \cdot x}{\int f(x,y)}$ 
[ ]: def barycentre (frame):
      X = np.linspace(1, frame.shape[0], frame.shape[0])
      centre_x = np.sum(np.sum(frame, axis=0)*X)/np.sum(frame)
      centre_y = np.sum(np.sum(frame, axis=1)*X)/np.sum(frame)
      return (centre_x,centre_y)

from a centro-symetric image, compute the azimuthal average
[ ]: def az_average(frame,center):
      x,y=np.indices(frame.shape)
      r=np.hypot(x-center[0],y-center[1])
      r=np.round(r)
      azimuthal=ndimage.mean(frame,labels=r,index=np.unique(r)[:666])
      return azimuthal
```

To compute $\langle \hat{N}(\mathbf{k}_\perp) \rangle$ from a recovery field:

```
[ ]: def N_k(frames):
      N_km=0 #initialize
      Em=np.average(np.abs(frames[0]))    #average of all fields
      dE=0
      for frame in frames:
          dE=dE+(frame-Em)/Em
      dE=dE/frames.shape[0]    #mean value
      a_k=np.fft.fft(dE)
      N_k=np.abs(a_k)**2
      return N_k
```

To compute the nonlinear refractive index n_2

```
phase=np.angle(data[0])-np.angle(data[0][int(barycentre(data[0])[0])][int(barycentre(data[0])[1])])           ↻ ↑ ↓ ← →
phase=unwrap_phase(phase)           #method of skimage.restoration to fo 2D unwrapping between with a pi discontinuity
phase=az_average(phase,(433,408))
phase=phase[:120]      #crop to match the size of the beam
L=1e-2    #length in m
alpha=1/L*np.log(7.5/3)      #absorption
k0=2np.pi/(780e-9)
dphi=np.abs(np.max(phase)-np.min(phase))
P_tot=31e-3
ds=(3.451e-6)**2      #taille pixel
#conversion
I=np.abs(data[0][int(barycentre(data[0])[0])][int(barycentre(data[0])[1])])2*P_tot/(np.sum(np.abs(data[0])**2)*ds)
n2=alphadphi/(k0(np.exp(alphaL)-1)I) #in m^2/W
```